

ITA WTC 2015 Congress and 41st General Assembly
May 22-28, 2015, Lacroma Valamar Congress Center, Dubrovnik, Croatia

TBM Pressure Models: Calculation Tools

Author: Tiago Gerheim Souza DIAS, Ghent University, Belgium, tgsdias@gmail.com

Co-author: Adam BEZUIJEN, Ghent University, Belgium, adam.bezuijen@ugent.be

Topic: Mechanized Tunnelling in Development and Use

Summary: Mechanized tunnel construction in soft ground has evolved significantly over the last 20 years, especially on the matter of settlement control. This was achieved by guiding the TBM operation to control the main factors that induce soil displacements, namely the face pressure and the closure of the soil-lining void. Nowadays, TBMs can be operated within strict serviceability requirements. However, several mechanisms of the excavation cycle are still not taken into account when estimating the induced soil deformations. Therefore, it is important to properly model the processes around a TBM, but in order for such models to be assimilated in the state of practice, they should be combined in a design framework where the operational characteristics can be assessed together with the induced soil displacements and lining forces for different project conditions. This paper presents the first step of this general project by focusing on the tail void grouting pressures. A model for the grout flow is associated with a finite element model to calculate the induced soil displacements in a dynamic equilibrium between the boundary pressures and the soil-lining gap. These two elements are combined in a calculation tool with a user friendly input-output layout.

Keywords: *TBM, Grout Pressure, Grout Rheology, Finite Element Modelling*

1. Introduction

Mechanized tunnel construction in soft ground has evolved significantly over the last 20 years, especially on the matter of settlement control. This was achieved by guiding the TBM operation to control the main factors that induce soil displacements, namely the face pressure and the closure of the soil-lining void. Nowadays, TBMs can be operated within strict serviceability requirements. However, several mechanisms of the excavation cycle are still not taken into account when estimating the induced soil deformations.

The mechanisms around a TBM can be schematically divided in three components: face pressure, flow around the TBM and tail void grouting pressure (Bezuijen & Talmon, 2008). The face pressure is normally understood as a normal stress, which increases linearly with depth and that can be applied as total stress boundary to the excavation face through an impermeable soil mixture. It is also assumed that any stress increment above the pore pressure will only generate increments of effective stress while the pore pressure remains constant. The impermeable soil mixture is normally called a cake and it should be achieved by clogging the soil pores with slurry particles, in the case of an SPB (Slurry Pressure Balance), or foam bubbles, in the case of an EPB (Earth Pressure Balance). However, excess pore pressure in front of SPB (Bezuijen et al., 2001) and EPB TBM tunnels (Bezuijen, 2002) were measured, revealing that the ideal process of cake formation is not always achieved and depends on properties of the soil, the additives and the excavation speed (Bezuijen et al., 2005). The idea that the excavation fluids flow around the TBM was first proposed from the observation that the measured volume loss was smaller than the gap between the excavation and the TBM, suggesting that this gap does not close and that it should be filled with the excavation fluids. This indicated that the grout was not only flowing toward the lining but also towards the face. There is a natural gap between the excavated perimeter and the shield at the tail due to the tapered cone shape of the shield. This gap tends to close as the excavation converges. However, due to the high pressures from the face and the grouting, this gap can be sustained or even expanded (Bezuijen, 2007). The balance between the soil deformability, the gap width, which influences the dissipation of fluid pressure, and the boundary fluid pressures will determine the pressure distribution and the diameter of the excavated boundary around the TBM (Bezuijen, 2009). Finally, the distribution and time progression of grout pressures around the lining have been associated with the characteristics of viscosity and shear resistance of the fluid grout

(Talmon et al., 2001) as well as its consolidation mechanism in a permeable soil (Bezuijen & Talmon, 2003). The results illustrate that the lining equilibrium is an intricate process of a buoyant structure immersed in a pressurized viscous fluid with a certain yield strength that is flowing as it hardens and consolidates (Bezuijen et al., 2004). This process should be considered locally, evolving with time, and regarding the previously installed lining rings, that will act together, as a beam (Talmon & Bezuijen, 2013).

These models enable a conceptual understanding of the mechanism and main parameters that influence the process of the TBM interaction with the surrounding soil. However, they cannot be directly used to estimate the tunnel volume loss and settlement trough, which determine if the TBM can be operated within strict serviceability requirements of the surrounding structures. The soil displacement field is normally calculated by analytical or numerical methods. The former is mostly applied for deep tunnels with specific boundary conditions whereas the latter is better suited to the higher stress gradients present around shallow tunnels. However, the numerical modelling technique that is normally adopted for conventional tunnelling, namely the stress release factor, cannot cope with these different stress gradients, as the pressures around the TBM are not necessarily a factor (λ) of the soil initial stress state (Dias & Bezuijen, 2014). The stress release factor technique assumes that the stress state on the imaginary boundary surface of the excavation can be represented as a fraction (λ) of the stress path from the initial in-situ stress to a condition of zero normal and shear stress. A lined tunnel should support part of this path with a free boundary (λ) and after the lining is installed the remaining stress ($1-\lambda$) should be released and reach equilibrium with the lining. The soil-lining interaction and the lining rigidity will dictate the equilibrium state of the tunnel.

There have been different approaches to adapt the traditional technique to model TBM tunnels, some of which will be described hereafter. The first attempts used a displacement criterion to control the stress release factor. The stress release factor was increased until the induced converge matched the TBM gap and then the lining was activated (Rowe et al., 1983). Subsequent studies revised this gap parameter to account for the quality of workmanship, face protrusion and other tunnelling aspects. Years later Bernat et al. (1999) modelled the TBM excavations of the Lyons-Vaise metro by calibrating the stress release factors of an unlined tunnel with the measured tunnel crown displacements. A single partial stress release was compared to a cycle of stress reduction, an increase ($\lambda < 0$) representing the grout injection at the tail void and a final reduction. Ding et al. (2004) analysed the different TBM phases of the Osaka subway line by combining stress release factors with special interface and lining elements. The normal and tangential interface stiffness were calibrated by the properties of the fresh and consolidated grout. Two distributions of an internal pressure, representing the grout injection, were tested along with the stress release factors. Konda et al. (2013) modelled the different phases of the TBM by a set of internal pressure on the tunnel boundary together with a full stress release ($\lambda = 1$), which allowed the internal tunnel pressures to be determined with no relation to the in-situ stress.

Therefore, it is important to properly model the processes around a TBM, but in order for these to be assimilated in the state of practice, they should be combined in a design framework where the operational characteristics can be assessed together with the induced soil displacements and lining forces for different project conditions. This paper presents the first step of this general project by focusing on the tail void grouting pressures. A model for the grout flow is associated with a finite element model to calculate the induced soil displacements in a dynamic equilibrium between the boundary pressures and the soil-lining gap. These two elements are combined in a calculation tool with a user friendly input-output layout.

2. Methodology

The methods around this calculation tool will be presented in three sections: the grout rheological model, where the grout pressures are calculated; the finite element code, where the grout pressures are used as boundary conditions to calculate the soil displacement; and the spreadsheet framework where the results of the two models can interact until numerical equilibrium is achieved.

2.1 Grout Rheological Model

At this stage of the project, the grout is considered a Bingham plastic fluid. This material behaves

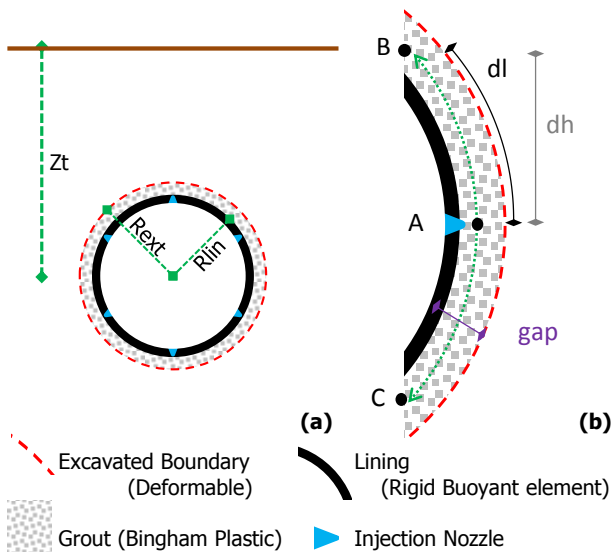


Fig. 1 Basic layout parameters (a) and details (b)

the shearing dissipation is connected to the flow direction and the flow path (dl) while the gravitational field depends on the vertical distance (dh) and the grout volumetric weight (γ_g). Normally, a TBM injection set-up consists of 6-8 injection nozzles. The simplest approach to deal with this is to calculate the grout pressure field around the tunnel for each individual nozzle and the resultant field will be the maximum pressure at each point around the tunnel.

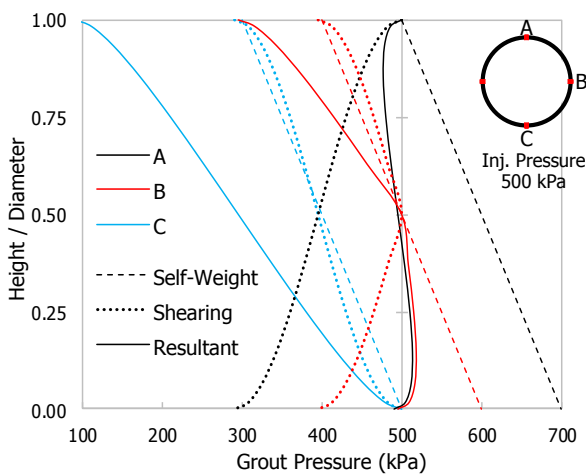


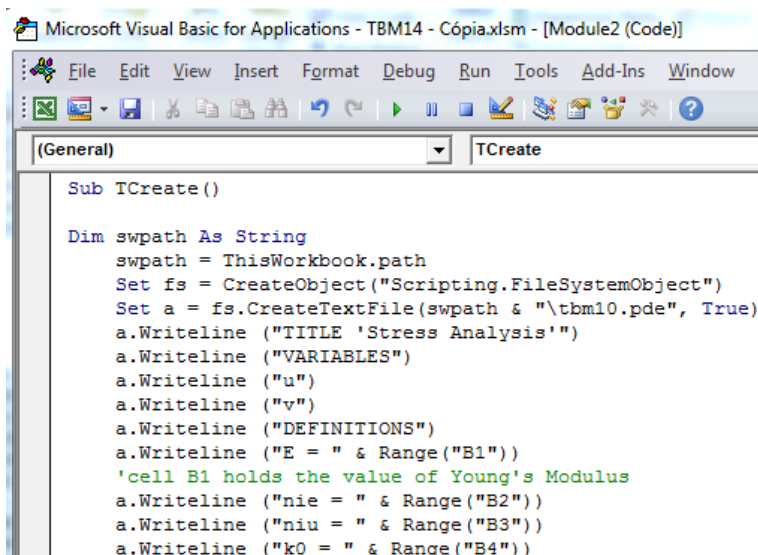
Fig. 2 Example of the profiles of grout pressures

For a more visual appreciation of this model, an example calculation was run through a constant gap of 15 cm, tunnel radius of 5 m, injection pressure of 500 kPa, grout yield strength of 2 kPa and unit weight of 20 kN/m³. The pressure fields of three nozzles, whose positions are illustrated in the figure, were divided by their gradients due to the shear stress and to the self-weight of the grout (Figure 2).

2.2 Modelling – FlexPDE

To solve the boundary value problem of a tunnel excavation regarding its mechanical equilibrium, the software FlexPDE, which is a general Partial Differential Equation (PDE) solver, will be used. The software uses the finite element and the finite difference methods for the solution of non-linear coupled systems. FlexPDE has friendly input and output features combined with automatic mesh generation, time-step control, and choice of non-linear approaches (PDE Solutions Inc., 2012). The general solvers, which are also called problem solving environments, tend to have a steep learning curve, and can potentially make the programming of stress-strain analyses a straightforward procedure. Its applications to geotechnical engineering have been mostly on unsaturated soil mechanics, slope stability and coupled thermo-mechanical problems (Gitirana Jr & Fredlund, 2003). The software operates over an input script that defines the necessary elements for the calculation, namely the definition of variables, parameters, partial differential equations, domain, boundary conditions and post-processing options. The code resembles a programming language even though it cannot cope with recursive procedures. This poses some difficulties in implementing incremental constitutive relations but it can easily cope with explicit models, as the linear elastic. The whole code has almost 300 lines and cannot be portrayed here for the lack of space, but the determinant parts will be described hereafter.

As a plane strain equilibrium calculation, the variables to be solved are the displacements on two



```
Microsoft Visual Basic for Applications - TBM14 - Cópia.xlsm - [Module2 (Code)]
File Edit View Insert Format Debug Run Tools Add-Ins Window
(General) TCreate
Sub TCreate ()
Dim swpath As String
swpath = ThisWorkbook.path
Set fs = CreateObject("Scripting.FileSystemObject")
Set a = fs.CreateTextFile(swpath & "\tbm10.pde", True)
a.Writeline ("TITLE 'Stress Analysis'")
a.Writeline ("VARIABLES")
a.Writeline ("u")
a.Writeline ("v")
a.Writeline ("DEFINITIONS")
a.Writeline ("E = " & Range("B1"))
'cell B1 holds the value of Young's Modulus
a.Writeline ("nie = " & Range("B2"))
a.Writeline ("niu = " & Range("B3"))
a.Writeline ("k0 = " & Range("B4"))
```

Fig. 3 Part of the VBA code

orthogonal directions, which are the same as used to define the domain. For this analysis a Cartesian XY system was chosen and the variables were named u for the X direction and v for the Y direction. The PDE's to be solved concern the equations in the X (Eq. 4) and Y (Eq. 5) directions. These equations are solved for the total normal stresses S_{xx} and S_{yy} and the shear stress S_{xy} . The out of plane stress can be computed from the S_{xx} and S_{yy} stresses. These stresses are related to three independent strain measures, namely the normal strains ϵ_{xx} (Eq. 6), ϵ_{yy} (Eq. 7) and the shear strain ϵ_{xy} (Eq. 8), through the elastic parameters K (bulk modulus) and G (shear modulus), as in Eq. 9, 10 and 11. As the three strain components

depend on the two problem variables (u , v) it is possible to solve the two variables with the two equations. These deformability parameters are assumed constant, setting a linear elastic model. The two elastic parameters can be manipulated to simulate undrained conditions, in a methodology similar to the one implemented in the PLAXIS software (Plaxis bv, 2013). The concept is that the bulk modulus (K) can be split into the components of effective stress (K_e) and pore water pressure (K_w), which are differentiated by the Poisson's ratio for drained (μ_e) and undrained (μ_u) conditions, which is close to 0.5. The shear modulus remains exclusively linked to the Young's modulus and the drained Poisson's ratio (See Eq. 12-15). For drained conditions, one must only set the $\mu_u = \mu_e$, which turns $K_e = K$ and $K_w=0$ that results in no increment of pore-pressures.

The points of connection between the grout model and the equilibrium calculation are the assessment of the soil-lining gap and the use of the grout pressures as the boundary conditions of the tunnel excavation. The gap can be calculated within the FlexPDE code through Equation 17, considering the difference between the radius of the deformable boundary ($x+u$, $y+v$) regarding the tunnel centre coordinates (X_t , Z_t) and the external lining radius (R_{lin}). The grout pressure is a stress boundary condition in the normal direction to the tunnel perimeter. However, all the parameters concerning directions in the code have to be defined along the directions of the problem's variables, in this case X and Y. Therefore, the grout pressure on the radial direction has to be converted into S_x (Eq. 18), S_y (Eq. 19) and S_{xy} (Eq. 20) so that it can be applied as a derivative boundary condition along the X (N_u , Eq. 21) and Y (N_v , Eq. 22) directions.

2.3 Calculation Tool – Excel

To combine the calculation of the grout pressures with the results (deformation) and the input (boundary conditions) of/for a FlexPDE calculation, an Excel spreadsheet with VBA macros is used. The FlexPDE script can be written with a simple VBA code for the generation of text files, reading the different parameters values directly from the Excel cells and saving the code as a .PDE file. The constitutive parameters of the soil, geometric characteristics of the tunnel, and grout pressures can be all automatically inserted in the FlexPDE scrip in this way. An example fragment of the code can be seen in Figure 3. The written script can be processed in FlexPDE through a *ShellExecute* command. The script can also include the set-up for exporting the GAP value and angular position, which can be imported back to Excel with a *QueryTables.Add.Connection* command. Another useful feature is the assessment of the net force acting on the lining, which together with the lining weight will cause the lining to move and/or to transfer forces to the adjacent segments.

Despite these time-saving procedures, a fundamental point of interaction of this framework is the detection of GAP closure between the soil and the lining. From the initial stress state, the boundary conditions are initially taken to a state of zero shear stress through a sequence of

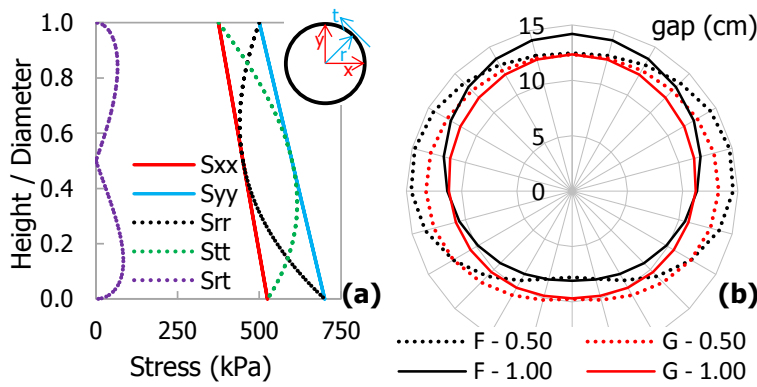


Fig. 4 Different components of boundary stress state (a) and resultant GAP from analytic equation and calculation tool (b)

coordinate transformations ($S_x, S_y, S_{xy} \rightarrow S_r, S_\theta, S_{r\theta=0} \rightarrow S_x, S_y, S_{xy}$), as it can be seen in Figure 4a. From this state, which normally induces minimal displacements, the boundary forces are incrementally taken to the grout pressure values, as in Equation 23, with the counter i is taken from 0 to k . This recursive code cannot be implemented in the scripting language of FlexPDE, but it poses no problem to

the VBA language. If GAP=0 is detected in any segment of the tunnel, herein divided in 15° segments, the counter i is stopped. This indicates

that soil-lining interaction is developing rather than the assumed soil-grout interaction. Around the rest of the tunnel the procedure can continue, although the flow conditions have to be adapted.

3. Examples and Discussion

In previous studies, the relation between the soil-lining gap and the grout pressure was assessed through a simple formula (Eq. 24) originally derived for isotropic conditions (Bezuijen & Talmon, 2003). An example calculation was performed to compare the analytic formula (G) with the present method (F) based on a finite element calculation (see Figure 4b). This example considers the following properties: SOIL - 45 MPa Young's modulus; 0.2 Poisson's ratio; 18 kN/m³ volumetric weight; drained analysis ($\mu_u = \mu_e$); and the water table at the surface. TUNNEL - 30 m depth; 5 m radius (R_{ext}), 4.85 m lining radius (R_{lin}). GROUT - 1.5 kPa yield strength; 18 kN/m³ volumetric weight. The results can be seen in Figure 4b for a uniform grout pressure of 300 kPa and two different coefficients of earth pressure at rest (K_0): 0.5 and 1.0. One can see that the average gap calculated by the present model and the analytical equation are very similar (≈ 11 cm). However, the finite element calculation captures the stress redistribution around the excavation. For $K_0=1$ this is pronounced at higher convergence on the invert in contrast to a higher gap on the tunnel roof. For $K_0=0.5$ the same occurs on the invert, while the higher gap is more pronounced on the tunnel springline.

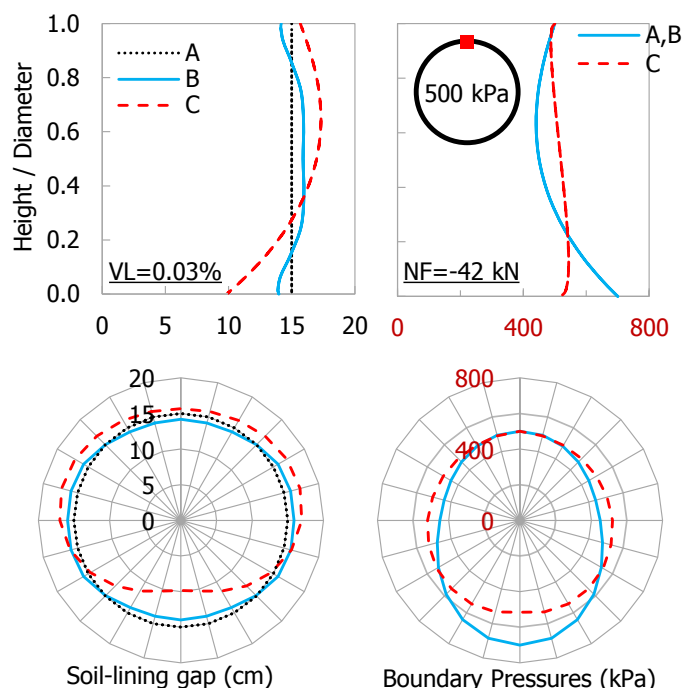


Fig. 5 Example with injection nozzle at the tunnel roof

All the parameters of the first example will be used in the following examples, with the exemption of the different injection pressures and layouts and that only $K_0=0.5$ is considered. The soil-lining gap and the boundary pressures are presented at three stages: A - initial stress state; B - initial stress state converged into normal stress ($S_r=0$); C - equilibrium with grout pressure profile. The injection strategy should aim at making state C as close as possible to state B in order to reduce the soil convergence and the consequent volume loss. As already discussed, the profile of grout pressures results from an intricate balance between the gap, yield strength, unit weight and injection strategy. Therefore, it is not an easy task to match the stress gradients of

the soil and the grout. The other side of this balance is the net force over the lining,

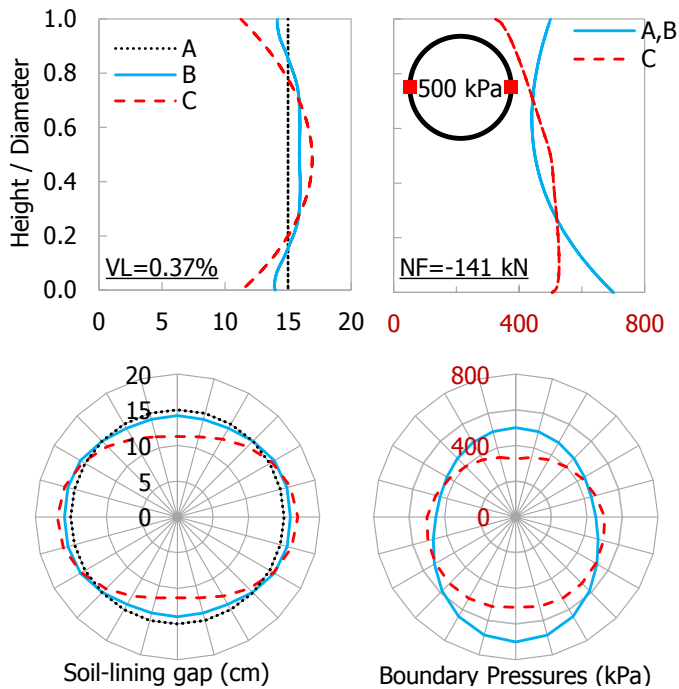


Fig. 6 Example with injection nozzle at the tunnel springline

is worth noting that this model does not consider the operational convenience of different injection systems. In this case, for example, the balance between the self-weight and the shearing dissipation of the grout pressure creates a relatively isotropic loading around the lining. Placing another nozzle at 500 kPa anywhere around the lining will barely change this distribution, so it is not analysed. However, extra nozzles can be needed to supply the necessary volumes to keep the soil-lining void pressurized while the TBM excavation advances. Even so, this model only considers how the nozzles do or do not affect the pressure distribution. The grout pressures are higher than the soil pressure from the top to about 20% the tunnel height. The effect of this can be seen at an expansion of the excavated perimeter (gap > initial gap) on the tunnel shoulders and a contraction on the tunnel invert. The difference is balanced quite well, resulting in a marginal volume loss of 0.03% on the tunnel boundary. This isotropic loading is also pronounced over a small net force of 42 kN acting upwards on the lining.

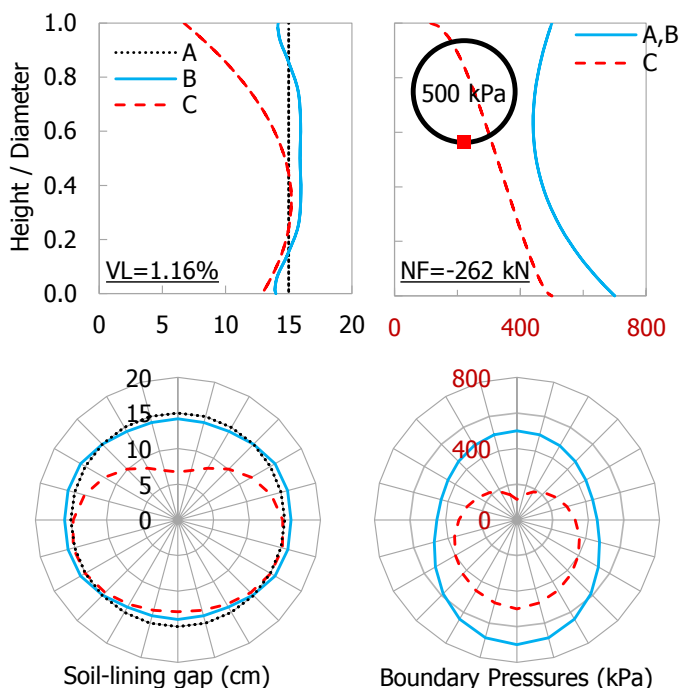


Fig. 7 Example with injection nozzle at the tunnel invert

which is smaller when a more isotropic pressure distribution is created. Another point to remark is that the volume loss measured on the tunnel boundary does not have the same volume as the settlement trough as long as the soil is compressible $\mu < 0.5$ and volumetric strains can develop. In this sense, a small volume loss just reflect a balance between expansion and contraction along the excavation perimeter, it does not mean that the displacement field around the tunnel is null. Three injection layouts will be tested: one nozzle at the roof, two at springline and one at the invert. All layouts will be tested with an injection pressure of 500 kPa.

Figure 5 presents the results of the first layout with the nozzle at the tunnel roof. It

is worth noting that this model does not consider the operational convenience of different injection systems. In this case, for

example, the balance between the self-weight and the shearing dissipation of the grout pressure creates a relatively isotropic loading around the lining. Placing another nozzle at 500 kPa anywhere around the lining will barely change this distribution, so it is not analysed. However, extra nozzles can be needed to supply the necessary volumes to keep the soil-lining void pressurized while the TBM excavation advances. Even so, this model only considers how the nozzles do or do not affect the pressure distribution. The grout pressures are higher than the soil pressure from the top to about 20% the tunnel height. The effect of this can be seen at an expansion of the excavated perimeter (gap > initial gap) on the tunnel shoulders and a contraction on the tunnel invert. The difference is balanced quite well, resulting in a marginal volume loss of 0.03% on the tunnel boundary. This isotropic loading is also pronounced over a small net force of 42 kN acting upwards on the lining.

Another possible strategy would be to place the injection nozzle at the tunnel springline. The same shear/gravity balance occurs from the nozzle downwards. However, both dissipation forces are combined upwards, decreasing the grout pressure on the tunnel roof. The resultant profile is somewhat the mirror projection of the soil stresses. As it can be seen in Figure 6, this becomes evident in the convergence profile with higher gaps along the springline and higher convergence on the roof and invert. The balance between convergence and expansion is not as good as in the previous example. The resultant volume loss is 0.37% and the net force on the lining is 141 kN acting upwards.

The last calculation places the injection nozzle at the tunnel invert (Figure 7). As in the previous case, there is significant pressure dissipation upwards towards the tunnel roof. This is pronounced in

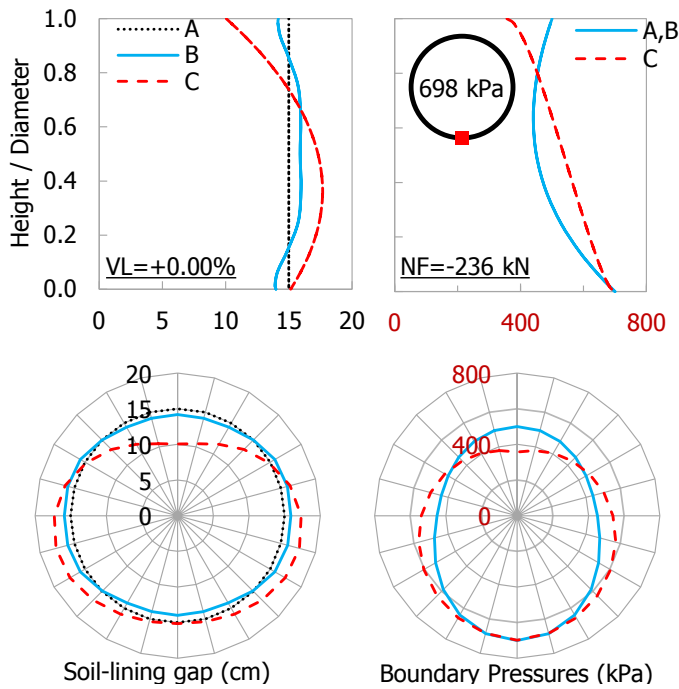


Fig. 8 Example with injection nozzle at the tunnel invert and higher injection pressure

considerable settlements at the tunnel roof and a much higher volume loss (1.16%). However, this should not be considered an implicit condition. Overall, this injection strategy is the one that most resembles the stress gradient of the soil initial stress. If the pressure is calibrated, in this case to about 700 kPa, the same pattern can result in a null volume loss, as it can be seen in Figure 8.

4. Conclusion

There have been significant advancements regarding how the processes around a TBM are understood and managed to achieve more reliable tunnel excavations. However, the quantitative models that represent these processes still feature as exceptional tools for the design of these tunnels, which includes the prediction of settlements.

This paper presented the first step of a general project to incorporate these models in the state-of-practice. A model for the grout flow was associated with a finite element model to calculate the induced soil displacements in a dynamic equilibrium between the boundary pressures and the soil-lining gap. These two elements were combined in a calculation tool with a user friendly input-output layout.

The model was used to compute different example situations and their consequences in terms of volume loss and net force on the lining. For a 500 kPa injection pressure, the layout with an injection nozzle on the tunnel roof resulted in the smaller settlements and lower net force. The worst case for this layout was re-calculated with a different injection pressure and resulted in a null volume loss. In all the cases, different soil and grout properties can turn the patterns described in the example section in different directions. However, the point of this study is that with an objective and accessible framework, any condition can be processed and the results evaluated in a few minutes.

Acknowledgements

The first author would like to acknowledge the financial support of the Brazilian Research Agency – CNPq.

Equations Appendix

$$\Delta p_g = \frac{\tau_y}{gap} . dl \quad (1)$$

$$p_B = p_A - \frac{\tau_g}{gap} . dl - \gamma_g . dh \quad (2)$$

$$p_C = p_A - \frac{\tau_g}{gap} . dl + \gamma_g . dh \quad (3)$$

$$\frac{\partial S_{xx}}{\partial x} + \frac{\partial S_{xy}}{\partial y} = 0 \quad (4)$$

$$\frac{\partial S_{xy}}{\partial x} + \frac{\partial S_{yy}}{\partial y} + f_y = 0 \quad (5)$$

$$\varepsilon_{xx} = -\frac{\partial u}{\partial x} \quad (6)$$

$$\varepsilon_{yy} = -\frac{\partial v}{\partial y} \quad (7)$$

$$\varepsilon_{xy} = -\frac{\partial v}{\partial x} - \frac{\partial u}{\partial y} \quad (8)$$

$$S_{xx} = S_{xx0} + \left(K + \frac{4.G}{3} \right) . \varepsilon_{xx} + \left(K - \frac{2.G}{3} \right) . \varepsilon_{yy} \quad (9)$$

$$S_{yy} = S_{yy0} + \left(K - \frac{2.G}{3} \right) . \varepsilon_{xx} + \left(K + \frac{4.G}{3} \right) . \varepsilon_{yy} \quad (10)$$

$$S_{xy} = S_{xy0} + G . \varepsilon_{xy} \quad (11)$$

$$G = \frac{E}{2.(1 + \mu_e)} \quad (12)$$

$$K = 2.G . \frac{(1 + \mu_u)}{3.(1 - 2.\mu_u)} \quad (13)$$

$$K_e = \frac{E}{3.(1 - 2.\mu_e)} \quad (14)$$

$$K_w = K - K_e \quad (15)$$

$$u_w = u_{w0} + K_w . (\varepsilon_x + \varepsilon_y) \quad (16)$$

$$gap = \sqrt{(x - Xt + u)^2 + (y + Zt + v)^2} - R_{lin} \quad (17)$$

$$S_{x_g} = p_g \quad (18)$$

$$S_{y_g} = p_g \quad (19)$$

$$S_{xy_g} = 0 \quad (20)$$

$$Nu = S_x . \cos(\theta) + S_{xy} . \sin(\theta) \quad (21)$$

$$Nv = S_{xy} . \cos(\theta) + S_y . \sin(\theta) \quad (22)$$

$$S = S_A + (S_B - S_A) \frac{i}{k} \quad (23)$$

$$\Delta \sigma = 2 \frac{\Delta r}{r} G \quad (24)$$

References

- [1] Bernat, S., Cambou, B. & Dubois, P. (1999). Assessing a soft soil tunnelling numerical model using field data. *Géotechnique*, 49(4): 427–452.
- [2] Bezuijen, A. (2002). The influence of soil permeability on the properties of a foam mixture in a TBM. *Geotechnical Aspects of Underground Construction in Soft Ground - 4th International Symposium (IS-Toulouse)*, Toulouse, France, 221–226.
- [3] Bezuijen, A. (2007). Bentonite and grout flow around a TBM. *ITA World Tunnel Congress 2007 - Underground Space – The 4th Dimension of Metropolises*, Prague, Czech Republic, 383–388.
- [4] Bezuijen, A. (2009). The influence of grout and bentonite slurry on the process of TBM tunnelling. *Geomechanics and Tunnelling*, 2(3): 294–303.
- [5] Bezuijen, A., Pruiksma, J.P. & van Meerten, H.H. (2001). Pore pressures in front of tunnel, measurements, calculations and consequences for stability of tunnel face. *International Symposium on Modern Tunnelling Science and Technology*, Kyoto, Japan.
- [6] Bezuijen, A. & Talmon, A.M. (2003). Grout, the foundation of a bored tunnel. *BGA International Conference on Foundations*, Dundee, Scotland.
- [7] Bezuijen, A. & Talmon, A.M. (2008). Processes around a TBM. *Geotechnical Aspects of Underground Construction in Soft Ground - 6th International Symposium (IS-Shanghai)*. CRC Press/Balkema, Leiden, Shanghai, China, 3–13.
- [8] Bezuijen, A., Talmon, A.M., Joustra, J.F.W. & Grote, B. (2005). Pressure gradients and muck properties at the face of an EPB. *Geotechnical Aspects of Underground Construction in Soft Ground - 5th International Symposium (IS-Amsterdam)*. CRC Press/Balkema, Leiden, Amsterdam, the Netherlands.
- [9] Bezuijen, A., Talmon, A.M., Kaalberg, F.J. & Plugge, R. (2004). Field measurements of grout pressures during tunnelling of the Sophia rail tunnel. *Soils and Foundations*, 44(1): 39–48.
- [10] Dias, T.G.S. & Bezuijen, A. (2014). Tunnel modelling: Stress release and constitutive aspects. *Geotechnical Aspects of Underground Construction in Soft Ground - 8th International Symposium (IS-Seoul)*. CRC Press/Balkema, Leiden, Seoul, South Korea, 197–202.
- [11] Ding, W.Q., Yue, Z.Q., Tham, L.G., Zhu, H.H., Lee, C.F. & Hashimoto, T. (2004). Analysis of shield tunnel. *International Journal for Numerical and Analytical Methods in Geomechanics*, 28(1): 57–91.
- [12] Gitirana Jr, G. & Fredlund, D.G. (2003). Analysis of transient embankment stability using the dynamic programming method. *56th Canadian Geotechnical Conference*, Winnipeg, Canada.
- [13] Konda, T., Nagaya, J., Hashimoto, T., Shahin, H.M. & Nakai, T. (2013). In-situ measurement and numerical analysis on tunnel lining and ground behaviour due to shield excavation. *3rd International Conference on Computational Methods in Tunnelling and Subsurface Engineering (EURO:TUN 2013)*, Bochum, Germany, 17–19.
- [14] PDE Solutions Inc. (2012). *FlexPDE Student Version 6.32s User Guide*. Washington, United States of America.
- [15] Plaxis bv. (2013). *Plaxis Material Models Manual*. Delft, The Netherlands
- [16] Rowe, R.K., Lo, K.Y. & Kack, G.J. (1983). A method of estimating surface settlement above tunnels constructed in soft ground. *Canadian Geotechnical Journal*, 20(1): 11–22.
- [17] Talmon, A.M., Aanen, L., Bezuijen, A. & van der Zon, W.H. (2001). Grout pressures around

a tunnel lining. International Symposium on Modern Tunnelling Science and Technology, Kyoto, Japan, 817–822.

- [18] Talmon, A.M. & Bezuijen, A. (2013). Analytical model for the beam action of a tunnel lining during construction. International Journal for Numerical and Analytical Methods in Geomechanics, 37(2): 181–200.